ELSEVIER

Journal of Crystal Growth 197 (1999) 355–363

JOURNAL OF CRYSTAL GROWTH

Equiaxed dendritic solidification in supercooled melts

Vladimir Pines[a], Arnon Chait[a,*], Marianne Zlatkowski[b], Christoph Beckermann[c]

[a] *Computational Microgravity Laboratory, NASA Lewis Research Center, Cleveland, OH 44135, USA*
[b] *Physics Department, Case Western Reserve University, Cleveland, OH 44106, USA*
[c] *Department of Mechanical Engineering, University of Iowa, Iowa City, IA 52242, USA*

Received 21 September 1998; accepted 23 September 1998

Abstract

The growth of equiaxed dendrites from a pure supercooled melt is examined. We propose modifications to the classical Ivantsov theory that allow for consideration of multiple interacting dendrites. The modified theory reveals the existence of a steady-state dendritic solidification mode in a frame of reference moving with the dendrite tip. This regime should be valid from the onset of nucleation to the commencement of time-dependent coarsening when the mass of the solid becomes comparable to the liquid mass in the solidification chamber. This regime is characterized by a reduced (relative to the single dendrite case) heat flux leading to slower solidification rates, but with the same level of supercooling. We study the effects of the relative proximity and number of interacting dendrites through a numerical example of solidification of succinonitrile, a common material used in many experiments. The data show that the model predicts a new steady growth regime that is different than the steady growth law of a single dendrite as described by Ivantsov theory.

PACS: 68.70. + w; 61.50.Cj

Keywords: Dendrite; Morphological instability; Solidification; Equiaxe

1. Introduction

Equiaxed dendrites are one of the most common growth morphologies in metal casting [1]. Equiaxed grains originate from small nuclei that are dispersed in a supercooled melt or attached to a mold wall. Usually, the free nuclei quickly develop instabilities at the solid/liquid interface and grow into equiaxed dendrites. Typical grain densities in cast materials range from 10^9 to $10^{15}/m^3$ and a fine equiaxed structure is often promoted through the use of inoculants or stirring [2]. Under conventional casting conditions, the supercoolings, and hence, the growth velocities are relatively small, resulting in diffusion lengths in front of the growing dendrites that can far exceed the spacing between the equiaxed grains. In that case, the dendritic growth stage that ensues after nucleation will be influenced by the presence of other grains. For high grain densities, the interactions can be so strong

* Corresponding author. Fax: + 1 216 433 5033; e-mail: chait@sarah.lerc.nasa.gov.

0022-0248/99/$ – see front matter
PII: S0022-0248(98)00901-4

from the beginning of growth that no dendritic branches can develop. The result is a globulitic microstructure consisting of spheroidal grains as is commonly observed in inoculated Al-alloy castings [3].

An understanding of the growth interactions occurring in equiaxed dendritic solidification is thus critical for the prediction of the resulting microstructure in cast materials. The interactions among multiple free equiaxed dendrites growing in a supercooled melt is the subject of the present investigation.

Existing theories of equiaxed solidification generally focus on the growth of isolated dendrites into an infinite supercooled melt. The most well-known result is due to Ivantsov [4], in which a similarity solution for the product of the tip radius and velocity is obtained as a unique function of the supercooling. This theory does not include the effect of capillarity, and thus cannot provide an adequate selection mechanism for separately calculating the tip radius and velocity. Incorporation of capillary effects in an expanded model of dendritic solidification (together with Ivanstov theory) has been proven to be exceedingly difficult to achieve, and competing theories have been introduced in Ref. [5].

In this work, we concentrate our attention to the problem of heat transfer in the presence of multiple dendrites only, i.e., we examine the modifications necessary to the Ivanstov theory alone. The case of multiple dendrites examined in this paper describes a particular experimental arrangement, and is a part of the more general case of equiaxed dendritic solidification. In this arrangement, the dendrites originate from the ends of small capillaries that are placed around the periphery of a spherical envelop and grow towards the common center. The number of multiple dendrites in such an experiment is a priori determined by the number of capillaries. In this work, we propose a modified Ivantsov theory that accounts for the presence of multiple dendrites under the specific experimental arrangement described above. The new solution is limited to small fractions of solid, and to diffusional transport of heat in pure materials. The physical considerations and assumptions on which the present model are based are detailed next. This is followed by a presentation of the model equations and parameters. Sample calculations are performed to illustrate the model results.

2. Physical considerations

We begin by considering the case of several dendrites that are solidifying in a supercooled melt and are pointing towards each other. The amount of heat of fusion generated by each actively solidifying dendrite is small. Compared with the large extent of the liquid and its heat capacity, that amount is insufficient to raise the bulk liquid temperature. Hereafter we define the liquid supercooling to denote the deviation of the bulk liquid temperature from the equilibrium melting temperature of a flat interface. It is important to realize that at this stage of growth, the supercooling as seen by any dendrite remains the same, namely, the difference between the dendrite tip temperature and the liquid bulk temperature. While the supercooling remains the same, the net heat flux at the dendrite interface, nondimensionally represented by the Péclet number, is changing. This point is not trivial, and it deserves further exposition.

The supercooling level is the same for all three cases: the classical Ivantsov (with the bulk temperature imposed at infinity), the Glicksman single dendrite experiments [6–10] (with the bulk supercooling applied at a fixed wall), and the case of multiple dendrites (with or without external walls). The supercooling will be the same provided that the bulk liquid mass is much larger than the solid mass. However, in each of these cases, the net heat flux at the dendrite interface is different. In the Ivantsov case, the heat flux corresponds to a temperature profile that asymptotes at infinity to the bulk liquid temperature. For a dendrite growing inside a finite chamber, with the bulk temperature being applied at its walls (Glicksman's experiment), the net heat flux is increased over the Ivantsov case. It simply represents the fact that the temperature distribution in the liquid ahead of the dendrite is different, giving rise to a steeper gradient in front of the dendrite tip. In the case under consideration (multiple dendrites), the gradient is reduced due to the increase in the local temperature between the dendrites. However, the latent heat which

is generated at all interfaces is conducted away from the dendrite interface into the liquid between the dendrites and is subsequently transported to the infinite bulk in a steady-state manner. The steady-state growth of dendrites in the scenarios described above can occur as long as the mass of the bulk liquid (its overall heat capacity) remains large in comparison with the solid. When the two are comparable, or when the solid mass is larger than the liquid mass, the bulk temperature would change in a time-dependent manner, and transient growth will ensue. The process is then referred to as coarsening. Indeed, Rappaz and Thevoz [11] and Wang and Beckermann [12] have recognized the need for using a raised bulk temperature in the Ivanstov model and have proposed earlier modifications to account for this effect.

Steady-state growth is the hallmark of dendritic growth into an infinite liquid. The existence of steady growth for wall-constrained or multiple dendrite cases is not that obvious. However, recent experimental observations imply the existence of steady-state growth for a single dendrite in a wall-constrained chamber. In careful diffusion-dominated experiments in microgravity, Glicksman and co-workers [6–10] have measured the dendrite tip radius and velocity at various supercooling levels for succinonitrile. The supercooling was applied on the experimental chamber wall at a finite distance from the dendrite. At low supercooling levels at which the diffusion length became greater than the distance to the wall, Glicksman's experimental setup essentially increased the heat flux at the interface by setting the value of the bulk supercooling at a finite distance from the dendrite rather than at infinity (see above). A nontrivial outcome from Glicksman's experiment was that the dendrites grew indeed at steady state (within experimental error), albeit at faster rates compared to the idealized Ivantsov case, with infinite extent liquid. That increase in solidification rate was due to the increase in net heat flux from the dendrite interface. Even more interesting was the observation that the solidification rate remained constant throughout the experiment, while the dendrite position relative to the wall was continuously changing. Only when the dendrite tip was very close to the wall did time-dependent growth replace the steady-state growth.

In the case under consideration (multiple dendrites), the net heat flux at the dendrite tip interface is decreased because of the increase in the inter-dendritic temperature at a finite distance due to the emission of latent heat from neighboring dendrites. An analogy with Glicksman's experiment suggests that the assumption of steady-state growth is plausible, and that the solidification rate should remain constant even while the dendrites approach each other. A departure from this behavior is only expected when the dendrite tips are very close, or when the mass of the solid becomes comparable or larger than the mass of the bulk liquid. In these cases the actual supercooling level is changing.

3. Model

Our model for interaction among dendrites is based on ideas originating from our previous analysis of dendrite–wall interaction [13]. In that study we extended the classical Ivantsov theory [4] that is valid for a single dendrite solidifying into an infinite extent supercooled melt to a more practical limit in which the supercooling is applied at a finite distance from the dendrite (e.g., container or experimental chamber wall). The possibility of constructing a steady-state similarity solution (in a frame of reference co-moving with the dendrite tip) in Ref. [13] is due to the modeling of the wall as a confocal paraboloid on which the supercooling is applied. Application of the model to Glicksman's diffusion-controlled dendritic growth data obtained in microgravity [6–10] has explained the entire range of supercooling used in the experiments, using a single additional parameter in the theory (wall proximity parameter). The apparent insensitivity of the physical diffusion process to the exact geometrical features of the wall (Glicksman's chamber was a rectangular box rather than a confocal paraboloid) is easily explained by the extreme 'near-sight' thermal vision of the dendrite, mathematically expressed by the Laplacian operator. It is the ability of the Laplacian to smooth out geometrical details that made the dendrite–wall model useful. In this study, we follow the same rational to include dendrite–dendrite interaction into the model.

The motivating example discussed above led us to consider dendrite–dendrite interactions in which the *details* of the dendrite surface itself are unimportant, as long as the physical heat transport processes are faithfully followed and certain geometrical parameters (e.g., the initial separation distance between dendrites) are kept in the model. Specifically, we wish to construct an imaginary envelope around any dendrite that would substitute for the heat generated by all neighboring dendrites. Each and every dendrite is solidifying with the same constant velocity since each is experiencing the same level of supercooling. To accomplish this purpose, the envelope must (a) generate the overall amount of heat generated by all neighboring dendrites, (b) be thermodynamically compatible (i.e., not disturb the continuity of the temperature field). Fig. 1 depicts such a region where the complex interfaces of the discrete neighboring dendrites are mapped onto a confocal paraboloid envelope. We require that the generation of heat of fusion on the envelop be equal to the total amount of heat generated by all neighboring dendrites. Written in a differential form, this requirement is formulated as

$$(\Delta q_n) \equiv q_n^{(+)}|_{r_q}(t) - q_n^{(-)}|_{r_q(t)} = \mu L V_n|_{r_q}(t) \tag{1}$$

where q_n is the heat flux, $+$ and $-$ refer to the two domains below and above the envelope, $\boldsymbol{r}_q(t)$ is the location of the envelope, V_n is the solidification velocity at the dendrite tip, μ is an interaction parameter that appears in the model as a consequence of mapping the complex neighboring dendrite interfaces onto the confocal paraboloid envelope (to be discussed later), and L is the heat of fusion per unit volume. The heat flux is defined by

$$\boldsymbol{q} = -k\boldsymbol{\nabla} T. \tag{2}$$

where k is the thermal conductivity and T is the temperature.

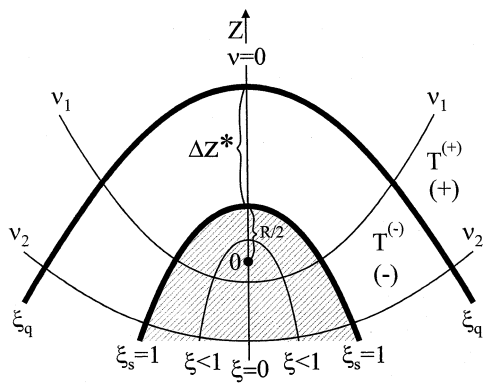

Fig. 1. Geometrical domain considered in the model.

It should be noted that the envelope is a fictitious interface that is situated in the modeling space. While it corresponds to the solid–liquid interface of neighboring dendrites in the physical space, it should not be thought of as a real solid–liquid interface. Consequently, the boundary conditions on the fictitious interface should be consistent with the heat transfer problem under consideration in the modeling space. Therefore, the only consistent boundary condition that is specified on the envelope, in addition to the heat flux jump condition in Eq. (1), is the continuity of temperature that is still unknown and must be solved for as a part of the solution:

$$T^{(+)}|_{r_q(t)} = T^{(-)}|_{r_q(t)}. \tag{3}$$

One additional note is warranted before we proceed with the derivation and solution of our model. The existence of steady-state solutions is a nontrivial aspect of solidification into a supercooled melt. Steady-state solutions are only found for a paraboloid that is solidifying such that its supercooling is constant with time. This requirement means that for both single and multiple dendrite cases the bulk temperature must be constant. This case may equally be valid when the liquid has either an infinite or a finite extent, as long as the mass of the bulk liquid is sufficiently large with respect to the solid mass. Therefore, steady-state growth is possible even with interacting dendrites that are moving with respect to each other in the laboratory frame, as long as the supercooling remains constant. The location of the fictitious interface in our modeling space is time-independent. This location could be computed from parameters in the physical space (as shown in the next section), but its independence of time in the modeling space is a direct consequence of the constant supercooling concept described here.

Our model considers the thermal fields in the two domains, one in between the imaginary envelope

surrounding a particular dendrite, and the other domain outside the envelope. In the following model we apply the supercooling at infinity; thus it is an extension of the classical Ivantsov model. The equations describing the thermal fields in the two domains are

$$\frac{\partial T^{(+)}}{\partial t} = \alpha_{\mathrm{L}} \nabla^2 T^{(+)}, \tag{4}$$

$$\frac{\partial T^{(-)}}{\partial t} = \alpha_{\mathrm{L}} \nabla^2 T^{(-)}, \tag{5}$$

where α_{L} is the thermal diffusivity of the liquid. The boundary conditions on the real dendrite interface represent the balance of energy and the local thermodynamic equilibrium. The balance of energy is represented as before via

$$(\Delta q_n) \equiv q_n^{(-)}|_{r(t)} = LV_n|_{r(t)} \tag{6}$$

where $r(t)$ is the location of the dendrite interface. Since the real dendrite is isothermal (at the melting temperature) as in the Ivantsov as well as in the present analyses, the heat of fusion must be conducted into the melt. Similarly, local thermodynamic equilibrium on the real dendrite interface is simply modeled as

$$T^{(-)}|_{r(t)} = T_{\mathrm{m0}}, \tag{7}$$

where T_{m0} is the equilibrium melting temperature of a flat interface. The supercooling T_∞ is applied at infinity:

$$T_l^{(+)}|_\infty = T_\infty. \tag{8}$$

These equations and boundary conditions are next written in a parabolic coordinate system (ξ, v, ϕ) co-moving with the tip velocity V:

$$x = R\xi^{1/2} v^{1/2} \cos\phi, \tag{9}$$

$$y = R\xi^{1/2} v^{1/2} \sin\phi, \tag{10}$$

$$z = \frac{R}{2}(\xi - v) + Vt, \tag{11}$$

where R is the tip curvature radius of the dendrite, and

$$0 \leqslant \xi \leqslant \infty, \tag{12}$$

$$0 \leqslant v \leqslant \infty, \tag{13}$$

$$0 \leqslant \phi \leqslant 2\pi. \tag{14}$$

We denote the locations of the parabolic dendrite interface and the surface of the imaginary envelope in the parabolic coordinates by $\xi_{\mathrm{s}} = 1$ for the real dendrite and by $\xi_q = \Omega_q$ for the imaginary envelope, (see Fig. 1). Hereafter the parameter Ω_q will be referred to as the proximity parameter. In Cartesian coordinates these locations are obtained by substituting the above values for ξ in Eqs. (9)–(11). To complete our model we nondimensionalize the temperature as

$$T = T_{\mathrm{m0}} + \left(\frac{L}{c_{\mathrm{L}}}\right)\theta, \tag{15}$$

where c_{L} is the specific heat of the liquid. The supercooling is defined as

$$\Delta \equiv \frac{(T_{\mathrm{m0}} - T_\infty)}{(L/c_{\mathrm{L}})}. \tag{16}$$

The solution for the above set of equations and boundary conditions provides an expression for the nondimensional net heat flux on the dendrite interface as the Péclet number, $P = VR/2\alpha_{\mathrm{L}}$:

$$P \cdot \mathrm{e}^P E_1(P) + \mu\Omega_q P \mathrm{e}^{\Omega_q P} E_1(\Omega_q P) = \Delta. \tag{17}$$

When $\Omega_q \to \infty$ we recover the classical Ivantsov solution because $\mu \to 0$ as $1/\Omega_q$ (see Eq. (18)).

4. The parameter μ

The parameter μ could be described as an interaction parameter that allows for the mapping of all solidifying interfaces generating latent heat onto the imaginary confocal parabolic interface surrounding the single dendrite under consideration. It should be proportional to the number of neighboring dendrites seen by the single dendrite, and should carry information about the actively solidifying region of the neighboring dendrites that influence the local net heat flux at the single dendrite interface.

In general, the parameter μ could be evaluated from experiments by fitting Eq. (17) to the data, with μ being the only free parameter, since Ω_q is computed from the geometrical configuration of the interacting dendrites as shown in the next

section. However, its structure can also be examined by performing the following simple analysis.

The parameter μ is evaluated by requiring the total heat generation rate on the imaginary envelope in our model to be equal to the total heat generation rate by all neighboring dendrites. The total heat generation on the imaginary envelope is calculated by integrating the local net heat flux, Eq. (1), over the surface of the parabolic envelope (see also Fig. 1). The total heat generated by all neighboring dendrite is obtained by integrating the local net heat flux, Eq. (6), over the single parabolic dendrite surface, multiplied by the number of neighboring dendrites, $(N-1)$. By equating the two expressions we obtain the μ parameter:

$$\mu = \frac{v(N-1)}{\Omega_q}, \tag{18}$$

where N is the total number of dendrites and v is a geometric form factor, $v \sim \mathrm{O}(1)$. The geometric form factor is introduced into the expression to signify the deviation of a real dendritic surface from the ideal parabolic shape analyzed in this study.

5. The parameter Ω_q

The presence of neighboring dendrites should begin to affect the thermal field produced by the dendrite when their diffusion lengths would overlap. As will be shown below, the diffusion length, defined as

$$l_{\mathrm{d}} = \frac{\alpha_{\mathrm{L}}}{V} \tag{19}$$

is an appropriate length scale for the extent of the thermal field in front of the dendrite. Before embarking on a technical description of how the parameter Ω_q is calculated, it is worthwhile to consider its physical origins.

For the case under consideration, in which the dendritic mass is much smaller than the bulk liquid mass, we distinguish between two fundamental scenarios:

1. The initial separation distance between the dendrites, l_q, is larger than the diffusion length, i.e., $l_q > 2l_{\mathrm{d}}(\Delta)$, or in terms of supercooling, $\Delta > \Delta^*$, where Δ^* is the critical supercooling when $l_q = 2l_{\mathrm{d}}(\Delta^*)$. This case essentially corresponds to the Ivantsov case since the thermal fields are clearly independent of each other. Since l_{d} is a characteristic distance at which thermal effects are sensed by the dendrite, then the presence of other dendrites outside l_{d} cannot be felt by the dendrite. The cessation of steady-state growth occurs when the dendrites get so close to each other that the process of heat transport to the bulk is hindered. This stage is marked by time-dependent coarsening.

2. The initial separation distance between the dendrites is smaller than the diffusion length, i.e., $l_q < 2l_{\mathrm{d}}(\Delta)$. In this case the dendrites never grow in an unconstrained Ivantsov mode since their growth is effectively dominated by an intermediate liquid temperature to be determined in this model. It is important to note that the supercooling does not change since heat is transferred to the large mass of liquid that is maintained at the bulk temperature. The presence of the intermediate region among the dendrites lowers the heat flux but not the supercooling. As in the previous case, only the onset of time-dependent coarsening marks the end of this steady growth.

The cornerstone of this analysis is the recognition that if the dendrites grow according to the second case, then the only additional parameter of importance in the model should be l_q. This parameter distinguishes between the two growth regimes. In the modeling space, this parameter is expressed via Ω_q, and the condition of $l_q = 2l_{\mathrm{d}}(\Delta^*)$ should provide the means to calculate its particular value.

We begin by considering the temperature profile between the interacting dendrites, $\theta(\xi)^{(-)}$, obtained by solving the field equations in Section 3:

$$\theta(\xi)^{(-)} = -\int_0^{P(\xi-1)} \frac{P\mathrm{e}^{-u}}{P+u}\mathrm{d}u$$

$$= -\int_0^{\Delta Z/l_{\mathrm{d}}} \frac{P\mathrm{e}^{-u}}{P+u}\,\mathrm{d}u, \tag{20}$$

where ΔZ is a distance measured along the parabolic coordinate line $v = 0$ from the tip of the paraboloid which is located at $R/2$ away from the origin of the parabolic coordinate system (see

Fig. 1 and Eq. (11)):

$$\Delta Z \equiv z(v=0,\xi,t) - \left(\frac{R}{2} + Vt\right) = \frac{R}{2}(\xi - 1) = l_d P(\xi - 1). \quad (21)$$

The upper limit for the integral is obtained using a simple substitution of the definition of ΔZ (Eq. (21)). Differentiating the temperature profile $\theta(\xi)^{(-)}$ from Eq. (20) with respect to ΔZ leads to

$$\frac{\partial\theta(\xi)^{(-)}}{\partial(\Delta Z)} = -\frac{1}{l_d}\frac{Pl_d}{Pl_d + \Delta Z}e^{-\Delta Z/l_d}. \quad (22)$$

At the dendrite tip, $\Delta Z = 0$ (i.e., $\xi = 1$, $v = 0$), the temperature derivative becomes

$$\left.\frac{\partial\theta(\xi)^{(-)}}{\partial(\Delta Z)}\right|_{\Delta Z=0} = -\frac{1}{l_d}. \quad (23)$$

From Eqs. (22) and (23) it is clear that l_d is a characteristic distance for the temperature drop.

We expect the interaction between neighboring dendrites to become significant when their diffusion lengths overlap. This overlap must occur simultaneously in both modeling and physical spaces. At an arbitrary separation distance, e.g., the initial separation distance among neighboring grains (l_q), we can find a specific level of supercooling (Δ^*) at which the overlap takes place. In physical space the overlap condition could be written as:

$$2l_d^* \equiv 2l_d(\Delta^*) = l_q. \quad (24)$$

In the modeling space the overlap condition is formulated as (see Fig. 1):

$$l_d^* = \Delta Z^* \equiv \Delta Z(\xi = \Omega_q). \quad (25)$$

Solving Eqs. (24) and (25) we can obtain an expression for the proximity parameter, Ω_q. Using the definition of l_d from Eq. (19) and the scaling law for V from Ref. [14]:

$$V = \frac{2\alpha_L}{d_0}\sigma P^2 \quad (26)$$

with d_0 being the capillary length and σ the scaling parameter, we formulate the diffusion length, l_d, as

$$l_d^* = \frac{d_0}{2\sigma P^2(\Delta^*)}. \quad (27)$$

Substituting l_d^* from Eq. (27) into Eq. (24) results in

$$\frac{1}{P(\Delta^*)} = \left(\frac{l_q\sigma}{d_0}\right)^{1/2}. \quad (28)$$

The expression for ΔZ^* in Eq. (25) (see also Fig. 1) follows from Eq. (21):

$$\Delta Z^* = l_d^* P(\Delta^*)(\Omega_q - 1). \quad (29)$$

Substituting l_d^* from Eq. (27) and ΔZ^* from Eq. (29) into Eq. (25) results in the following simple relation between Ω_q and $P(\Delta^*)$:

$$\Omega_q = 1 + \frac{1}{P(\Delta^*)}. \quad (30)$$

Finally, substitution of $P(\Delta^*)$ from Eq. (28) into Eq. (30) gives the expression for the proximity parameter, Ω_q as

$$\Omega_q = 1 + \left(\frac{l_q\sigma}{d_0}\right)^{1/2}. \quad (31)$$

In practical cases, the parameter Ω_q could be evaluated from the grain density, n, by simply substituting $l_q \to n^{-1/3}$.

It is interesting to note that the expression for Ω_q should be also valid for analyzing Glicksman's single dendrite experiments [6–10] in which the solidification process was performed inside a finite size container. As discussed before, the overlap in physical space is specific to the particular case under examination. For equiaxed dendrites this condition is expressed by Eq. (24). For the single dendrite case the overlap condition should occur when the diffusion length became equal to the radius of the container, R_w : $l_d(\Delta^*) = R_w$, because the dendrite was initiated from the center of the container. For that particular case, simple algebra leads to the expression for Ω (corresponding to Ω_q in this study) discussed in Ref. [13] similar to Eq. (31) where l_q is replaced by $2R_w$. For $R_w \sim 1.1$ cm, approximately corresponding to the average radius of the container used in the experiments, and for SCN material parameter $d_0 = 2.65\times10^{-7}$ cm, Eq. (31) with $l_q \to 2R_w$ and $\sigma = 0.0192$ yield $\Omega = 400$. This value was taken for the value of Ω in Ref. [13] and was shown to fit the experimental data over the entire range of supercooling.

6. Discussion

To illustrate the influence of the various parameters in the model, we present results calculated from this model for succinonitrile (SCN) in an infinite supercooled melt. This transparent organic material is extensively used as a model material for solidification experiments, and its material properties are well documented [10].

We begin by examining in Fig. 2 the effect of four interacting dendrites ($N = 4$) on the heat transfer, with the interaction proximity parameter $\Omega_q = 100$. The particular value of this parameter corresponds to an initial dendrite separation distance of about $l_q \sim 1.5$ mm. This separation distance corresponds to grain density of $n \sim 1/l_q^3 \sim 3 \times 10^8/\mathrm{m}^3$. Throughout the remainder of this discussion the parameter v was assigned a value of unity. We expect the actual value of v to be less than one. Its particular value could be determined from experiments. As expected, the Péclet number (the nondimensional net heat flux at the interface) for the multiple dendrite case is consistently lower than that for the single dendrite.

The effect of the interaction proximity parameter, Ω_q, is further examined in Fig. 2 for the case of $N = 4$ interacting dendrites. Since Ω_q is proportional to the square root of the relative distance between the locations of the onset of the dendrites, $\Omega_q = 400$ thus corresponds to about 15 times that distance for $\Omega_q = 100$ case, namely, $l_q = 2.2$ cm.

Varying the number of dendrites in the model has a profound effect on the heat transfer. As expected, the ability of each dendrite to efficiently transfer its heat of fusion to the bulk is severely hampered by the existence of neighboring dendrites. Indeed, doubling the number of the interacting pairs of dendrites ($N - 1$, where N is the total number of dendrites) in Fig. 3 produces an almost proportional effect in the heat transfer, albeit a smaller effect at the high supercooling levels.

To further illustrate the importance of interactions among dendrites, we present in Figs. 4 and 5 the dendrite tip radius and solidification velocity, respectively, for $N = 4$ and $\Omega_q = 100$. Unfortunately, the use of a constant scaling parameter, σ to calculate both R and V is not supported by experimental data [6–10]. Subsequently, Pines et al. [14,15] have shown, using scaling arguments, that the following expansion is sufficient to describe all of Glicksman's single dendrite data for R and V [6–10]:

$$\sigma(\Delta) = \sigma_2 + \frac{\sigma_1}{P(\Delta)}. \tag{32}$$

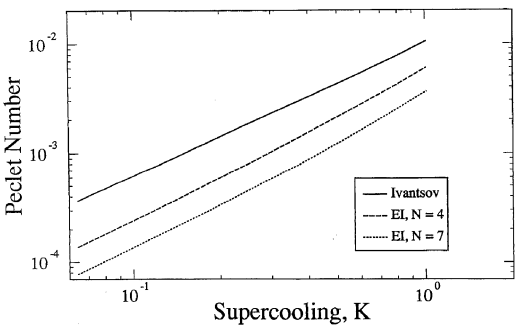

Fig. 3. Effect of number of interacting dendrites with $\Omega_q = 100$.

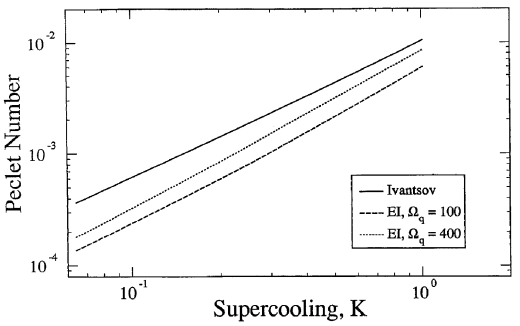

Fig. 2. Comparison between the single dendrite Ivantsov theory and predictions from this model for $N = 4$ and $\Omega_q = 100, 400$. EI refers to Equiaxed Ivantsov.

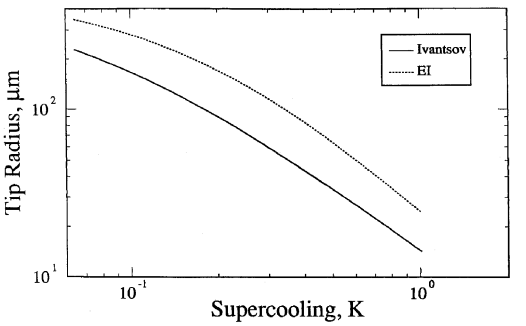

Fig. 4. Dendrite tip radius predicted for a single dendrite using Ivantsov theory and from the present theory with $N = 4$ and $\Omega_q = 100$.

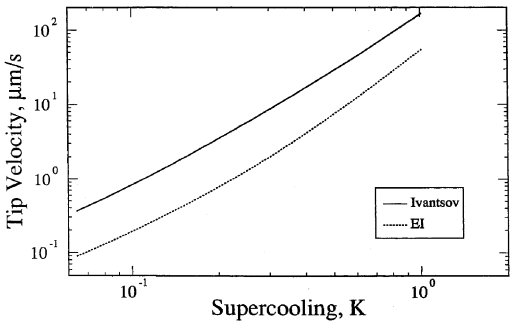

Fig. 5. Dendrite tip velocity predicted for a single dendrite using Ivantsov theory and from the present theory with $N = 4$ and $\Omega_q = 100$.

Using this relationship, Eq. (31) becomes

$$\Omega_q = 1 + \frac{l_q\sigma_1}{2d_0} + \sqrt{\left(\frac{l_q\sigma_1}{2d_0}\right)^2 + \frac{l_q\sigma_2}{d_0}}. \tag{33}$$

In calculating the radius and velocity we used the scaling parameters [14] with $\sigma_1 = 5.3 \times 10^{-6}$, $\sigma_2 = 0.0172$ as obtained from a fit to Glicksman's data [6–10]. We postulate that, in the absence of convection and mass transport, the selection parameters would not be different for the multiple dendrite case since the interaction among dendrites should only affect the diffusive heat transfer process.

In this work we presented an extension of the classical Ivantsov theory that is valid for a single dendrite in a supercooled bath to the more practical case of multiple interacting dendrites. The results demonstrate the existence of a steady-state growth regime. It is anticipated that the results presented here would be valid throughout the solidification process, commencing with the nucleation of dendrites and ending with the onset of a time dependent coarsening regime when the solid mass becomes comparable to the mass of the liquid phase.

Acknowledgements

This work is supported by the Microgravity Science and Applications Program of NASA and by the Materials Division of the Office of Naval Research. The authors wish to thank Thomas Glasgow and Henry de Groh for their useful discussions and Dr. Francis Chiaramonte for suggesting this problem to us (V.P., M.Z. and A.C.). One of the authors (C.B.) acknowledges the support of NASA contract NCC8-94.

References

[1] W. Kurz, D.J. Fischer, Fundamentals of Solidification, 3rd ed., Trans Tech Publ., Aedermannsdorf, Switzerland, 1992.
[2] D.G. McCartney, Int. Mater. Rev. 34 (1989) 247.
[3] M. Rappaz, Int. Mater. Rev. 34 (1989) 93.
[4] G.P. Ivantsov, Dokl. Akad. Nauk SSSR 58 (1947) 567.
[5] M.E. Glicksman, S.P. Marsh, in: D.J.T. Hurle (Ed.), Handbook of Crystal Growth, vol. 1, Pt. b, Elsevier Science Publishers, Amsterdam, 1993, p. 1077.
[6] M.E. Glicksman, M.B. Koss, E.A. Winsa, Phys. Rev. Lett. 73 (4) (1994) 573.
[7] M.E. Glicksman, M.B. Koss, L.T. Bushnell, J.C. LaCombe, E.A. Winsa, ISIJ International 35 (6) (1995) 1216.
[8] M.E. Glicksman, M.B. Koss, L.T. Bushnell, J.C. LaCombe, E.A. Winsa, MRS Fall Meeting, Symp. P, Boston, MA, 1995, in press.
[9] M.E. Glicksman, M.B. Koss, L.T. Bushnell, J.C. LaCombe, in: M. Cross, J. Campbell, (Eds.), Modelling of Casting, Welding, and Advanced Solidification Processes VII, The Minerals, Metals, and Materials Society, 1995.
[10] M.E. Glicksman, M.B. Koss, L.T. Bushnell, J.C. LaCombe, Private communication.
[11] M. Rappaz, Ph. Tevoz, Acta Metall. 35 (1987) 1487.
[12] C.Y. Wang, C. Beckermann, Metall. Trans. A 24A (1993) 2787.
[13] V. Pines, A. Chait, M. Zlatkowski, J. Crystal Growth 167 (1996) 383.
[14] V. Pines, A. Chait, M. Zlatkowski, J. Crystal Growth 167 (1996) 777.
[15] V. Pines, A. Chait, M. Zlatkowski, J. Crystal Growth 182 (1997) 219.